Chemical Engineering Journal 156 (2010) 40–48

Contents lists available at ScienceDirect

Chemical Engineering Journal

journal homepage: www.elsevier.com/locate/cej

Effect of increasing anode surface area on the performance of a single chamber microbial fuel cell

Mirella Di Lorenzo[b,*], Keith Scott[b], Tom P. Curtis[a], Ian M. Head[a]

[a] School of Civil Engineering and Geosciences, Newcastle University, Newcastle upon Tyne, United Kingdom
[b] School of Chemical Engineering and Advanced Materials, Newcastle University, Newcastle upon Tyne NE1 7RU, United Kingdom

ARTICLE INFO

Article history:
Received 21 May 2009
Received in revised form
16 September 2009
Accepted 18 September 2009

Keywords:
Microbial fuel cell
Wastewater
Tubular reactor
Bio-anode
Air cathode
Graphite granules

ABSTRACT

The anode material and its configuration represent an important parameter in a microbial fuel cell (MFC), as it influences the development of the microbial community involved in the electrochemical bio-reactions.

The aim of this work was to evaluate single chamber microbial fuel cells (SCMFCs) with high anode surface area, achieved by using packed beds of irregular graphite granules. The performance of the SCMFC with the packed bed anode configuration was studied using a mixed microorganism culture from real wastewaters in batch and continuous mode operation.

The current output was found to increase with the increase in thickness of the anode bed and with the approximate anode area. The best performance was obtained with the 3 cm anode bed depth SCMFC. When the latter was operated in batch mode, Coulombic efficiencies varied from 30% to 74%, depending upon feed COD. In continuous mode operation, the COD removal was 89% and Coulombic efficiency 68% with a feed COD of 50 ppm, and at a flow rate of 0.0028 $cm^3\ min^{-1}$. Power performance was also reasonable with a volumetric power density of 1.3 $W\ m^{-3}$, with respect to the net anodic volume (12.5 cm^3). Comparable performance was achieved with real wastewater. Over the duration of tests current output was stable. The investigation performed in this study represent a step forward for implementing real applications of MFC technology. A model of the current distribution in the packed bed electrode was applied, which correlates the effective utilization of the electrode to its specific area, solution conductivity and slope of the polarization curve. This model could function as a starting point in designing appropriate electrode geometries.

1. Introduction

Microbial fuel cells (MFCs) represent a particular case of fuel cells in which the direct conversion of chemical into electrical energy is due to the action of biocatalysts.

The attractiveness of this novel technology is related to the wide range of potential applications, including the possibility of achieving energy recovery from wastewaters [1]. In addition MFCs have been considered for hydrogen production [2,3], sulphide removal [4], and as biosensors for organic content in wastewaters [5–8].

Many MFC devices utilizing specific axenic cultures have been developed [8–12], however, MFCs operated with mixed cultures show higher resistance against process disturbance, larger substrate versatility and also higher power output [13,14].

Since the first application of the two chamber design, the configuration of MFCs has been continuously optimized. Moreover, improved electrode materials and better understanding of bacterial community involved in the electrochemical reactions, have led to ever increasing performance [15–19].

The maximal current generated with MFCs is still very low, being only of 0.1 A, and the average power density of MFCs is about 40 $W\ m^{-3}$, when operated in batch mode and fed with a synthetic effluent [20].

Actually, the major obstacles for practical applications of MFCs in a wastewater treatment plant concerns mainly difficulties in the scaling-up process and the very high capital costs [21].

The anode material and its configuration represent an important parameter in an MFC, for it influences the development of the microbial community involved in the electrochemical reactions.

In particular, a three-dimensional anode would allow a greater surface area for microbial attachment and therefore improve anode potential. Graphite granules have been widely used as both anode and cathode material [4,16,22,23]. Several other type of three-dimensional anodes have been previously tested such as

* Corresponding author. Present address: National Nanotechnology Laboratory, CNR-INFM, Distretto Tecnologico ISUFI, Università del Salento via Arnesano, I-73100 Lecce, Italy. Tel.: +39 0832298120; fax: +39 0832298146.
E-mail address: Mirella.Dilorenzo@unisalento.it (M. Di Lorenzo).

1385-8947/$ – see front matter © 2009 Elsevier B.V. All rights reserved.
doi:10.1016/j.cej.2009.09.031

reticulate vitreous carbon, granular activated carbon, carbon foam and graphite brush electrodes [17,24–26]. In general the power production has shown to increase with higher surface area materials [24].

Recently, Aelterman et al. [27] proved the benefits of a three-dimensional anode, by analyzing the electrochemical performance of two-chambered MFCs characterized by five different three-dimensional anodes. Liu et al. [28] and Zhang et al. [29] have reported performance of MFC with packed bed anodes. Liu et al. used acetate as the feed and an inoculum from a wastewater. Zhang et al. MFC tests were made with a pure culture (*Klebsiella pneumoniae* strain 117) and volumetric power densities were reported using an air cathode.

In this work, we evaluated the effect of increasing anode surface area to reactor volume ratios on the performance of a single chamber microbial fuel cell (SCMFC). The increase in anode surface area was achieved by using packed beds of irregular graphite granules with a mean size of 0.3 cm. Three different granule bed depths were in particular considered, 0.3, 1, and 3 cm, whilst a graphite plate anode was used as a one-dimensional point of comparison. A preliminary model of the current distribution in the packed bed electrode was also applied to the MFC, in which the effective utilization of the electrode was correlated to its specific area, electrode thickness, solution conductivity and slope of the polarization curve.

2. Materials and methods

2.1. Microbial fuel cell and its operation

The single chamber microbial fuel cells (SCMFC) were made from polyacrylate tubes, 4 cm inner diameter, 4 cm length. The cells had three flow ports (each 1.0 cm diameter); one at the bottom and two on the top (see Fig. 1). The port at the bottom was used for the inlet, one at the top for the outlet and one was used for the reference electrode. The open volume of the anode chamber was 50 cm^3.

To determine the effect of anode surface area on the performance of the SCMFC an anode made of graphite pellets (diameters between 0.2 and 0.6 cm, Carbon International, London, UK) was used. The pellets were packed inside the anode to occupy a defined fraction of the reactor. A circular piece of titanium net (12.5 cm^2 cross-sectional area) was used to separate the granules from the bulk solution and to provide an electrical connection. A titanium wire (0.1 cm diameter), passing through the middle of granule bed and connected to the titanium net, was also used. By adjusting the position of the titanium net it was possible to fill different volumes of the reactor anode chamber with graphite pellets to provide anodes with a range of surface areas. In this work, the SCMFC used three thicknesses of granules: 0.3, 1 and 3 cm bed depth. This gave total anode volumes (Va_{tot}) of approximately 3.75, 12.5 and 37.5 cm^3, respectively. The anode cross-sectional area was 12.5 cm^2 whilst the total anode surface area (Sa_{tot}) increased with the pellet layer thickness, and was calculated by approximating the area of a single pellet with the surface of a sphere having an average diameter of 0.4 cm and by multiplying the surface of one pellet into the total number of pellets introduced in the reactor. The estimated total anode surface areas, with this assumption, were 90 cm^2 for a 0.3 cm layer of pellets; 499 cm^2 in the case of a 1 cm layer and 1247 cm^2 in the case of a 3 cm layer (calculations are based on the actual number of granules used). This approximation did not consider the contribution of the pellet roughness to the Sa_{tot} nor its internal porosity.

The cathode was exposed to air on one side and on the other it was separated from the anode by a cation exchange membrane (Nafion® 117, DuPont). The cathode was a carbon supported platinum catalyst (0.3 mg Pt cm^{-2}; 60% on Vulcan, E-tek), deposited on wet proofed (20 wt% Teflon) Toray carbon paper from E-tek. The cross-sectional area was 12.5 cm^2.

In this study the anode and cathode were connected through a voltmeter (Pico® data logger) and an external resistance was applied to polarise the cell and monitor the current variation under closed circuit conditions. The external resistance was controlled by utilizing a resistor substitution box (RS 500, 1% accuracy, Elenco Electronics).

During the test in continuous mode, wastewater was fed through the injection port at a flow rate ranging from 0.03 to 1 $cm^3\ min^{-1}$ using a peristaltic pump (Watson-Marlow, 520S) equipped with Marprene II tubing (0.14 cm internal diameter). The MFCs were operated at room temperature which was approximately $21 \pm 2\ ^\circ C$. Each experiment was performed in duplicate.

2.2. Fuel

The fuel was an "artificial" wastewater (AW) made with the following constituents: NH_4Cl, 40 mg dm^{-3}; $MgCl_2$, 10 mg dm^{-3}; $CuSO_4$, 0.1 mg dm^{-3}; $CaCl_2$, 5 mg dm^{-3}; $MnSO_4$, 0.1 mg dm^{-3}; $ZnCl_2$, 0.1 mg dm^{-3}; phosphate buffer (1.0 mol dm^{-3} (M), pH 7);

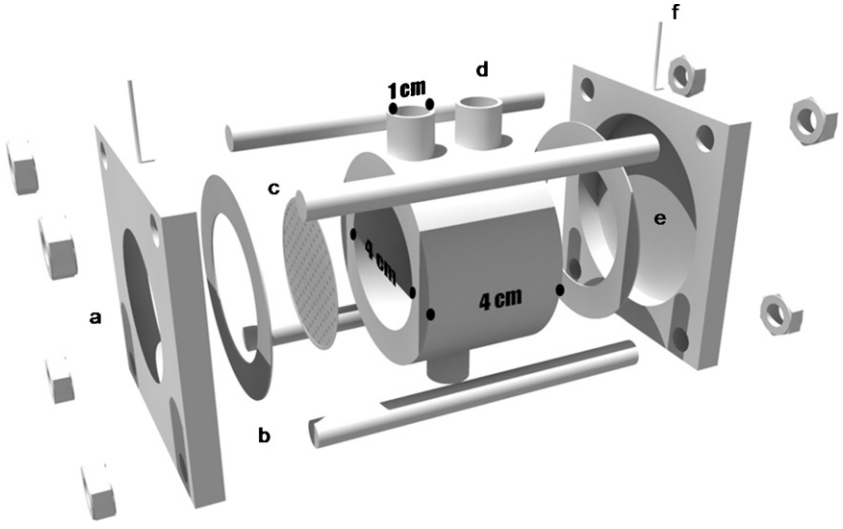

Fig. 1. Schematic diagram of the SCMFC biosensor system. Single chamber microbial fuel cell. (a) cathode side; (b) gasket; (c) titanium net; (d) inlets; (e) anode side; and (f) connection wire (titanium).

Table 1
Characteristics of the wastewater utilized.

Parameter	Value
pH	7
Alkalinity, mg dm^{-3}	46 ± 3
Conductivity[a], μS cm^{-1}	1570 ± 10
COD, mg dm^{-3}	175 ± 50
BOD, mg dm^{-3}	88 ± 5
TOC, mg dm^{-3}	98 ± 2
NH_3-N, mg dm^{-3}	21 ± 0.3
Phosphate, mg dm^{-3}	4.1 ± 0.9
Sulphate, mg dm^{-3}	49.4 ± 9
Total suspended solids, mg dm^{-3}	187 ± 18

[a] At 20.7 °C.

and distilled water. The COD concentration of the AW was controlled by adding an appropriate amount of glucose. The AW was autoclaved at 121 °C for 10 min prior to use.

Treated wastewater (WW) was collected from the primary clarifier of the wastewater treatment system at Cramlington treatment plant (Northumbrian Water, UK). The wastewater was collected during a period of heavy rain and had a COD of 175 ± 50 mg dm^{-3} (ppm) and other characteristics shown in Table 1. It was collected in one batch and stored at 4 °C until use and its COD did not markedly change during storage. To prevent clogging of the microbial fuel cell, the WW was filtered with a woven cloth prior to use.

2.3. Enrichment

The enrichment and adaptation of the electrochemically active bacteria in the SCMFCs was performed in batch mode under a fixed external load of 500 Ω, and was carried out for a period of approximately 4 weeks. A COD of 1000 ppm (mg dm^{-3}) was used for enrichment and anaerobic sludge (collected from the treatment plant of Cramlington, UK) was added as a bacterial inoculum. Once a stable peak current was observed, the cells were fed with AW with a COD of 200 mg dm^{-3} and no inoculum.

2.4. Analyses

We based the analysis on chemical oxygen demand (COD), since it was equal to the BOD for the artificial wastewater, and more conveniently measured than BOD_5. The COD was determined by the standard method using chromate as the oxidant as previously described [30].

The percentage of COD removal was calculated with the formula:

$$\frac{COD_{in} - COD_{out}}{COD_{in}} \times 100\% \quad (1)$$

where COD_{in} (mg dm^{-3}) was the COD of the influent and COD_{out} (mg dm^{-3}) was the COD of the effluent. In the case of MFC operation in continuous mode COD_{out} represented the COD of the effluent at the steady-state.

Total suspended solids of the wastewater from primary clarifier were determined as previously described [31].

Sulphate and phosphate concentration were determined using a Dionex ICS-1000 ion chromatograph with an AS40 automated sampler and with an IonPac AS14A, 4 mm × 125 mm analytical column; a 8-mM Na_2CO_3 solution was used as eluent at a flow rate of 1 cm^3 min^{-1}. A sample loop of 25 μL was used; the detector was an electrochemical conductivity detector.

The Coulombic efficiency (fractional), was calculated with the formulas (2) and (3), in the case of operation in continuous and batch mode operation, respectively:

$$\varepsilon_c = \frac{MI}{FzQ\Delta COD} \times 100\% \quad (2)$$

$$\varepsilon_c = \frac{MC}{Fzv\Delta COD} \times 100\% \quad (3)$$

where F is Faraday's constant (96,485 C mol^{-1}); M = 32 the molecular weight of oxygen, I (A) the current at the steady-state; z = 4 the number of electron exchanged per mole of oxygen, Q (dm^3 s^{-1}) the flow through the system, ΔCOD (g dm^{-3}) the difference in the influent and effluent COD, C charge passed (A s), v (dm^3) the anodic volume. Current integration with time to calculate the Coulombs was performed with the rectangular method.

Conductivity measurements were performed with a conductivity meter provided by Hanna instruments.

The internal resistance was measured by electrochemical impedance spectroscopy using a potentiostat (Gillac, ACM Instruments) with the cathode as the working electrode and the anode as counter electrode and reference electrode. Impedance measurements were conducted at open circuit voltage (OCV) over a frequency range of 10^4 down to 10^2 Hz with a sinusoidal perturbation of 15 mV amplitude.

Polarization curves were recorded by means of a potentiostat (Gillac, ACM Instruments) at a scan rate of 1 mV s^{-1} and a prior open circuit potential of over 4 h.

2.5. Current distribution model

To obtain a preliminary analysis of the required thickness (L) of a packed bed graphite granule anode, a basic mathematical model of the current and potential distribution was developed.

The simple model of current distribution in a packed bed microbial fuel cell anode is based on the assumption that both the electrode and electrolyte are continuous and Ohm's Law applies in both phases. The thickness of the electrode is L. The total current density at any cross-section in the direction of current flow between the anode and cathode is the sum of the current densities in the electrolyte solution phase (i_s) and the electrode phase (i_m):

$$i = i_m + i_s \quad (4)$$

and thus i is constant:

$$\frac{di_m}{dx} + \frac{di_s}{dx} = 0 \quad (5)$$

where x (in cm) is the electrode dimension measured from the point of current collection (x = 0) to the interface between the packed bed electrode and the membrane or free solution, i.e. the thickness of the electrode (x = L).

By applying Ohm's Law in both phases we have

$$i_m = -\sigma \frac{dE_m}{dx} \quad (6)$$

$$i_s = -\kappa \frac{dE_s}{dx} \quad (7)$$

where κ and σ are the effective conductivities (S cm^{-1}) of the electrode and solution phases, respectively, and E_s is the potential of the solution phase and E_m the potential of the electrode phase (V).

The variation of reaction rate in the packed bed electrode depends upon the specific kinetics of the electron exchange reaction as given by

$$-\frac{di_m}{dx} = a \times \text{function}[(E_m - E_s),\ C] \quad (8)$$

where a is the specific area of the electrode (cm^{-1}), $(E_m - E_s)$ is the electrode potential (V) and C is the reactant species concentration (mol cm^{-3}).

For this preliminary model we assume that linear kinetics apply (applicable to low overpotentials) and that species concentrations

are constant, therefore:

$$-\frac{di_m}{dx} = \frac{di_s}{dx} = c \times (E_m - E_s) \quad (9)$$

where c (Ω^{-1} cm^{-1}) is a constant.

The value of c can be described from the linear approximation of the Butler–Volmer kinetic equation for electrode kinetics or from the slope of an electrode polarization curve measured for a specific MFC anode.

In the first case, from the Butler–Volmer equation:

$$i = i_0 \left[\exp\left(\frac{\alpha nF}{RT}(E_m - E_s)\right) - \exp\left(-\frac{(1-\alpha)nF}{RT}(E_m - E_s)\right)\right] \quad (10)$$

where i_0 is the exchange current (A); E is the electrode potential (V); T the absolute temperature (K); n the number of electrons involved in the electrode reaction; F is Faraday's constant (96,485 C mol^{-1}); R the universal gas constant (8.314 J K^{-1} mol^{-1}); and α the so-called symmetry factor, dimensionless.

The term c is given by

$$c = a \times i_0 \frac{nF}{RT} \quad (11)$$

Assuming the symmetry factor $\alpha = 0.5$.

On the other hand, for an experimental polarization curve of an anode which has a slope of s (S cm^{-2}), the results is $c = as$

Differentiating Eq. (9) gives

$$\frac{d^2 i_s}{dx^2} = c\frac{d(E_m - E_s)}{dx} \quad (12)$$

Substituting Eqs. (6) and (7) for the derivative of E_s and E_m gives

$$\frac{d^2 i_s}{dx^2} = -c\left(\frac{i}{\kappa} - i_s\left(\frac{1}{\kappa} + \frac{1}{\sigma}\right)\right) \quad (13)$$

The solution to this differential equation is

$$\frac{i_s}{i} = \frac{\kappa}{(\kappa+\sigma)}\left[1 + \frac{(\sigma/\kappa)\sinh(\nu(1-y)) - \sinh(\nu y))}{\sinh(\nu)}\right] \quad (14)$$

where $y = x/L$ and $\nu = L[c((1/\kappa) + (1/\sigma))]^{0.5}$.

Under the conditions where $\sigma \gg \kappa$, i.e. for a wastewater with conducting electrodes, Eq. (14) simplifies to

$$\frac{i_s}{i} = \frac{\sinh[\nu(1-y)]}{\sinh(\nu)} \quad (15)$$

To analyse the effect of scaling up the electrode thickness we adopted the concept of effectiveness, which defines the utilization of the electrode area according to the definition [32]:

$$\eta = \frac{\text{observed current}}{\text{current obtained if the electrode potential was equal to the maximum observed at position } L \text{ in the electrode}}$$

The current flowing into the electrode at $x = L$ is defined by the gradient of the solution phase current density:

$$\frac{di_s}{dy}|_{y=1} = i\frac{\nu}{\tanh(\nu)} \quad (16)$$

The effectiveness is thus given by

$$\eta = \frac{\tanh(\nu)}{\nu} \quad (17)$$

Thus, the utilization of the electrode area is a function of the specific area, electrode thickness, solution conductivity and slope of the polarization curve, s, i.e.:

$$\nu = L\left(\frac{as}{\kappa}\right)^{0.5} \quad (18)$$

where s is the polarization curve slope (S cm^{-2}), a the specific area of the electrode (cm^{-1}), and κ the effective conductivity of the electrolye (S cm^{-1}).

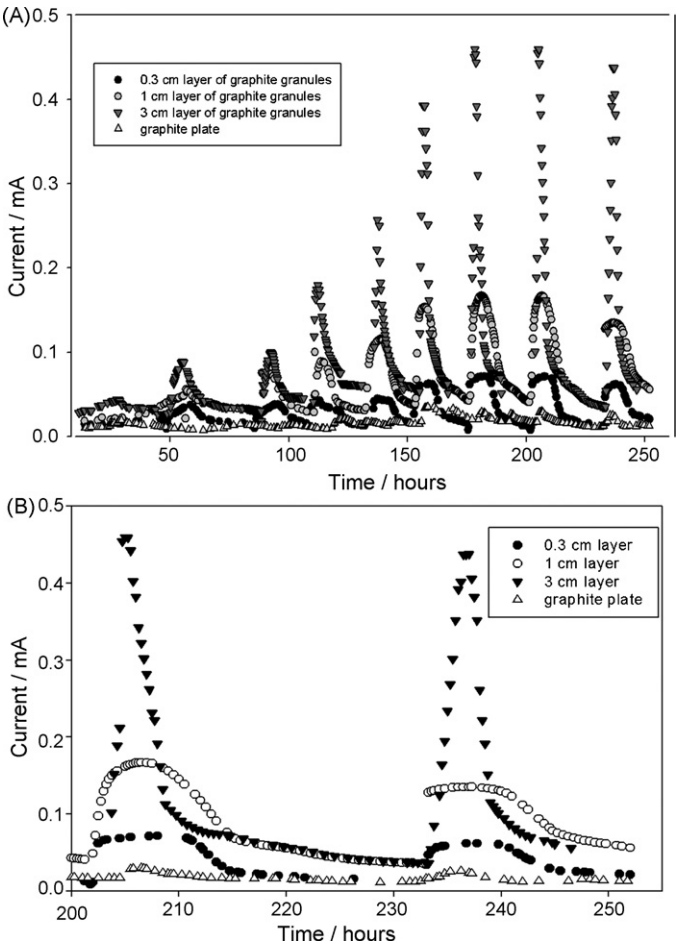

Fig. 2. Variation of current with time for electrochemically active bacterial enrichment of the SCMFCs. Data related to each anode configuration are the average from two reactors, 3% accuracy. Anode cross-sectional area: 12.5 cm^2. External resistance: 500 Ω. (A) The first 8 batches were performed with anaerobic sludge as inoculum (0.5% by volume) and AW (1000 ppm COD). The 9th batch was performed with AW containing 1000 ppm as COD and no inoculum. (B) Batches 8th and 9th.

In particular, for the MFC utilized in this study the values of the system parameters are $s = 1.0 \times 10^{-5}$ S cm^{-2} (from the polarization curve of a flat one-dimensional electrode), $a = 33$ cm^{-1}, and $\kappa = 1.57 \times 10^{-3}$ S cm^{-1}.

3. Results

3.1. Effect of increasing anode surface area to volume ratios on the SCMFC performance in batch mode operation

The performance of single chamber microbial fuel cells characterized by three different anode thicknesses (L equal to 0.3, 1, and 3 cm) were evaluated. In order to have a direct comparison with a one-dimensional electrode, a graphite plate anode was used for comparison.

Firstly, the anode biofilm of each reactor was enriched with electrochemically active bacteria as shown in Fig. 2, which reports current generation during the period of enrichment.

The relative current peaks varied with the surface area and, the 3 cm thick graphite granule anode gave the highest peak current. The differences between the peak currents increased with the num-

Table 2
Comparison of SCMFCs performance according to the anode configuration. Fuel: AW (1000 ppm as COD). R_{ext}: 500 Ω. Average from two reactors.

Layer of granules	Net anodic volume, cm^3	Internal resistance, Ω	Max current, mA	Max power density[a], $mW\,m^{-2}$	Max power density[b], $W\,m^{-3}$	COD removal, %	Coulombic efficiency, %
Graphite plate	50	128	0.027 ± 0.003	0.28	0.007	30 ± 4	0.8 ± 0.1
0.3 cm	46.2	128	0.063 ± 0.004	1.59	0.043	35 ± 1	6.5 ± 0.2
1 cm	37.5	104	0.16 ± 0.011	7.40	0.247	41 ± 5	5.3 ± 0.2
3 cm	12.5	5	0.450 ± 0.02	80.3	8.1	69 ± 1	30 ± 2

[a] With respect to the cathode cross area (12.5 cm^2).
[b] With respect to the net anodic volume.

ber of batches used. In the case of the first batch a difference of only 0.02 mA was observed, whilst after the 7th batch a difference between the anode configurations with bed depths of 0.3 and 1 cm was of 0.095 mA, and much higher (230%) between the 1 and 3 cm layer.

Following the enrichment period, when the SCMFCs were fed with AW containing 1000 ppm COD and no inoculum, the peak currents obtained were 0.45 mA with a 3 cm layer of pellets, 0.167 mA with a 1 cm layer of graphite pellets and 0.063 mA with a 0.3 cm layer of pellets, as reported in Table 2 and shown in Fig. 2A and B. The values of peak current almost scale-up in terms of the thickness of the bed and the anode surface areas. In the case of the 0.3 cm thick anode, which essentially consisted of a single layer of granules, the higher current (in comparison with graphite plate) was a result of the actual higher surface area, even allowing for any reduced utilization of this area due to current distribution behaviour.

According to Eq. (16), for the 1 cm thick electrode ($\nu = 0.49$) the estimated effectiveness in the electrode area utilization, "η", is equal to 0.92, whilst for the 3 cm electrode ($\nu = 1.35$) $\eta = 0.65$.

This estimation suggests that the 3 cm thick electrode should, under identical conditions, produce a current around 2.12 (i.e. $3 \times 0.65/0.92$) times higher than the current given by the 1 cm electrode. This is in reasonable agreement in terms of the measured peak currents in Table 2 and Fig. 2 where the ratio of the two peaks currents is 2.69 ± 0.2. For scaling up from 0.33 to 1.0 cm the currents should scale-up in proportion to the thickness increase which is in reasonable agreement with seen in practice. The particular feature of the packed bed systems in microbial fuel cells is that because current densities are very low then quite uniform current densities should be produced.

Clearly the model we described is very simple and ignores important factors. The effect of biofilm development over graphite granules is not considered, nor its distribution along the granules bed depth. These parameters, in combination with diffusion problems, are likely to lead to variation in local concentrations of substrate and therefore to an electricity production which is not spatially uniform along the anode. An initial improvement in the model would be to introduce a mass transport effect of substrate inside the packed bed electrode using Fickian diffusion. This will be the subject of work to be reported later.

The local generation of any microbial produced mediators was also not considered by our model. The mechanism of electron transfer by a biocatalyst has been deeply investigated in MFCs: for some electro-active bacteria, such as *Shewanella* and *Geobacter* species, it has been proposed to occur through highly conductive nanowires produced by the bacteria, whilst for other species, *Pseudomonas* species for example, it requires external mediators or electron shuttles [19]. A proper model would, therefore, take into account the efficiency of electron transfer to the electrode by analyzing the local availability of mediators, but this would mean a perfect knowledge of the electro-active fraction of the bacteria community developed on the granules and the mechanism of electron transfer that each bacteria would require. This is not feasible as the MFC environment has demonstrated to be suited for the growth of a large variety of microorganisms but a typical electricity generating microbial community has not been established yet [20].

Nevertheless, our model could function as a starting point in designing appropriate electrode geometries from basic knowledge of wastewater conductivity and preliminary biofilm electroactivity.

Apart from the approximations of our model, the difference we found between the experimental and theoretical values could in part be explained by the difference in geometries between the two reactors, for the 3 cm thick electrode had a lower internal resistance.

In fact, for the graphite plate anode and graphite granules anodes in layers of 0.3 and 1 cm, the differences in the internal resistances produced were minor: 128 Ω, for graphite plate and 0.3 cm layer, and 104 Ω for 1 cm layer of pellets (see Table 2). On the other hand, with a 3 cm layer configuration the internal resistance decreased to 5 Ω, due to the much shorter distance between anode and cathode [33]. Thus, a contributory factor in achieving the higher current, in this case, was the lower internal resistance and therefore lower Ohmic losses. What a lower internal resistance might do would be to increase the actual current flowing (and COD removed anodically) with the same external load. This would partly explain why the model currents, predicted through the effectiveness factor, were actually lower than the measured values.

The wastewater treatment performance improved with the thickness of the anode bed depth. The reactors with a 3 cm layer of granules in fact, led to 79% of COD removal, nearly 3 times higher than with the graphite plate anode. This is the consequence of an enhanced area for the development of biofilm involved in the COD biodegradation [17].

The higher anode surface area and the reduced internal resistance increased the Coulombic efficiency: switching from graphite plate to 3 cm graphite granules led to a Coulombic efficiency approximately 37 times higher.

3.2. *Performance of the SCMFC filled with a 3 cm layer of granules in batch mode and continuous mode operation*

Among the four anode configurations analyzed in this work, the 3 cm layer of graphite granule anode resulted in the best reactor performance, both from an electrochemical (current, power output and Coulombic efficiency) and a wastewater treatment efficiency (COD removal) point of view. We focused, therefore, on the SCMFC having this anode configuration and investigated the effect of the COD loading rate, comparing the two cases of batch mode and continuous mode operation.

In both cases, the COD loading rate was varied by feeding the system with artificial wastewater characterized by several inlet CODs.

Fig. 3 shows the typical MFC polarization and power density behaviour for the case of a 3 cm graphite granular bed. The open circuit potential was around 0.5 V and the peak power was 160 $mW\,m^{-2}$ at a current density of around 0.095 $mA\,cm^{-2}$ (~1.1 mA). In this data the major loss in power is due to anode polarization as shown in the measured potentials in the MFC. The

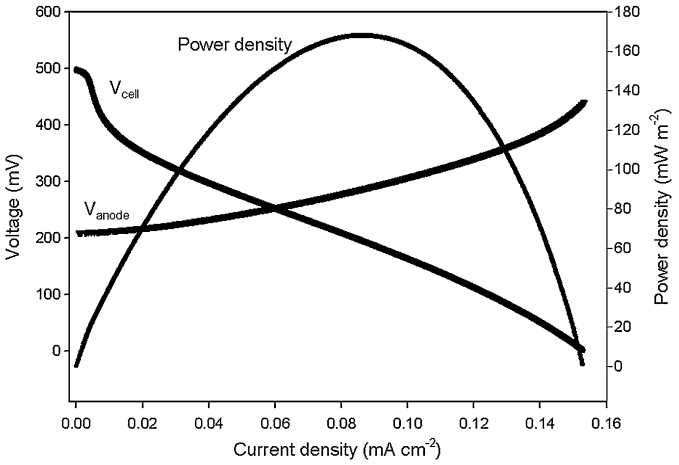

Fig. 3. Polarization and power density curves: anode—graphite granules (3 cm layer). Power and current density refers to the anode cross-sectional area: 12.5 cm^2. The polarization curves were recorded by means of a potentiostat (Gillac, ACM Instruments) at a scan rate of 1 mV s^{-1} and a prior open circuit potential of over 4 h. The cells were fed with AW containing 1000 ppm as COD.

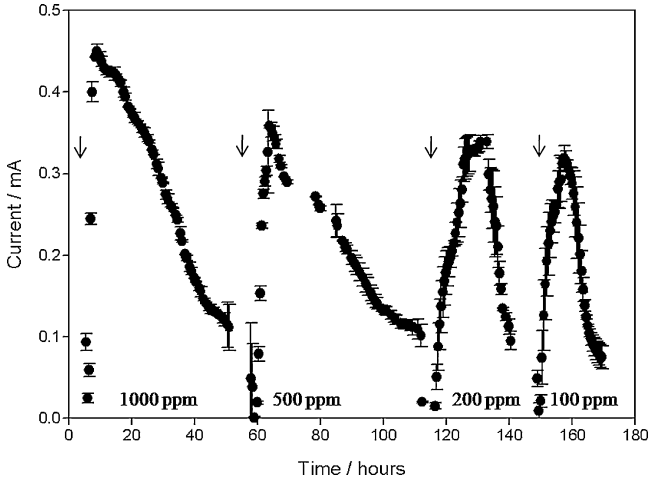

Fig. 4. Variation of current with time: anode—graphite granules (3 cm layer). Arrows indicate the point in which a new batch was performed at a COD concentration reported in the graph. R_{ext}: 500 Ω. Error bars refer to two reactors.

estimated loss in voltage from the internal resistance (5 Ω) would be around 90 mV at a current density of 0.15 mA cm^{-2}, indicating that the loss in potential at the cathode was small, not surprisingly with a Pt based electrode operating at low current density.

Table 3 and Fig. 4 reports the system performance for the case of batch mode operation. On one hand, a 10-fold reduction of the inlet COD caused a fall in the electrochemical performance of the system, characterized by a drop in the output current and power of approximately 31% and of 53%, respectively.

On the other hand, the Coulombic efficiency increased by decreasing the COD loading rate, reaching a value of 74% for a

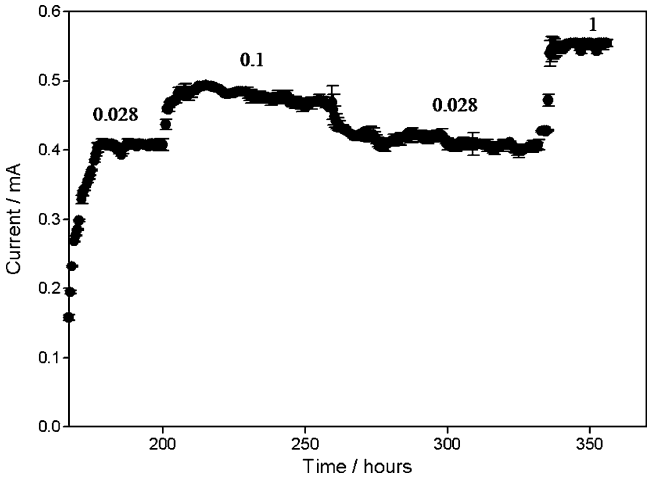

Fig. 5. Effect of the hydraulic retention time on SCMFC performance: variation of current with time. Anode: graphite granules (3 cm layer). Numbers indicate the AW flow rate in cm^3 min^{-1} utilized to feed the SCMFC. R_{ext}: 500 Ω. Error bars refer to two reactors.

feed COD equal to 100 ppm. Therefore, even if the overall COD removal percentage did not markedly change, the amount of COD removed by non-Faradaic reactions decreased from 48% for a COD_{IN} of 1000 ppm, to only 18% for a COD_{IN} of 100 ppm.

It is known that in MFCs methanogens compete with the electrochemically active microorganisms and convert organic material to methane, thus reducing electron recovery [21].

It was previously observed that at higher organic loading rates the Coulombic efficiency was reduced, and methanogenesis accounted for more organic carbon oxidation [16].

High COD loadings, corresponding to highly saturated conditions with respect to anode surface area, may lead to competition between microorganisms involved in electricity production and other types of bacteria, leading to greater COD removal not related to current generation and, consequently, lower Coulombic efficiencies. When the fuel concentration decreased, conditions became more favourable for the electrochemically active bacteria.

When the SCMFCs operation was switched from a batch mode to a continuous mode, firstly the effect of the hydraulic retention time (HRT) on the overall system performance was investigated. The aim was to subsequently perform the analysis in continuous mode at the HRT that demonstrated to be "optimal" for our system.

With this purpose, three flow rates were considered: 0.028, 0.1, and 1 cm^3 min^{-1} (see Table 4 and Fig. 5), whilst the inlet COD was kept constant at 200 ppm. The system was continuously fed at a specific flow rate until a steady value of the output current was obtained. Afterwards, a new value of the flow rate was used.

The effect of HRT was consistent as shown by the effect of the reduction in flow rate after the first increase from 0.028 to 0.1 cm^3 min^{-1}.

By increasing the flow rate the output current increased until a maximum of 0.55 mA for the case of a flow rate of 1 cm^3 min^{-1}; with a maximum increase of 33% when switching from 0.028 to 1 cm^3 min^{-1}. For each value of flow rate the output current was

Table 3
Effect of the COD loading rate in batch mode. Graphite granule bed depth: 3 cm. Fuel: AW. R_{ext}: 500 Ω.

Inlet COD, ppm	Max current, mA	Max volumetric power density[a], W m^{-3}	Maximum power density, mW m^{-2}	COD removal, %	Coulombic efficiency, %	COD removed by non-Faradaic reaction, %
1000	0.450 ± 0.009	8.1	81	69 ± 1	30 ± 2	48
500	0.354 ± 0.007	4.9	49	62 ± 3	57 ± 5	27
200	0.331 ± 0.005	4.4	44	60 ± 5	76 ± 2	14
100	0.312 ± 0.009	3.8	38	68 ± 4	74 ± 1	18

[a] With respect to the net anodic volume (12.5 cm^3).

Table 4
Effect of the hydraulic retention time (HRT) on the SCMFC performance. Graphite granule bed depth: 3 cm. Fuel: AW with 200 ppm of COD. R_{ext}: 500 Ω.

Flow rate, $cm^3\ min^{-1}$	HRT, min	Current output at the steady-state, mA	Power output at the steady-state, mW	Coulombic efficiency, %	COD removal, %
0.028	446	0.413 ± 0.007	0.085 ± 0.004	63 ± 4.5	69 ± 5.2
0.1	125	0.478 ± 0.008	0.114 ± 0.005	44.3 ± 7	31.3 ± 4.6
1	12.5	0.55 ± 0.004	0.151 ± 0.003	7.4 ± 1.9	19.9 ± 4.1

higher than in the case of a batch mode operation (i.e. higher than 0.331 mA), which was presumably due to the effect of a reduced COD levels in the batch experiment at the peak current point.

The system response to HRT increment depend on the step size, as shown in Fig. 5: switching from a flow rate of 0.028 to 1 $cm^3\ min^{-1}$, required 4 h for a stable current output, whilst for the change from 0.028 to 0.1 $cm^3\ min^{-1}$ only half of the time (i.e. 2 h) was needed. The response to a flow rate decrease (from 1 to 0.028 $cm^3\ min^{-1}$) was slower than the case of the respective increase (from 0.028 to 1 $cm^3\ min^{-1}$), requiring approximately twice the time (i.e. ~4 h vs 2 h).

As expected, by decreasing the fluid retention time and, in other words, the time available by the bacterial community to digest the fuel, the COD removal decreased and reached the lowest value of 19.9% at 1 $cm^3\ min^{-1}$.

The Coulombic efficiencies also decreased with the increase in flow rate, and in general, for each HRT considered, they were lower with respect to the operation in batch mode, with major differences for low HRTs. A flow rate of 0.1 $cm^3\ min^{-1}$, gave in fact a Coulombic efficiency 1.71 times lower than operation in batch mode, whilst when the system was fed at 1 $cm^3\ min^{-1}$, the Coulombic efficiency was 10 times lower.

In conclusion, even though the highest current and power output was observed at 1 $cm^3\ min^{-1}$, the best Coulombic efficiency and COD removal were observed at the lowest flow rate, 0.028 $cm^3\ min^{-1}$, with values, respectively, of 63% and 69%. For this reason, we consider the flow rate of 0.028 $cm^3\ min^{-1}$ as suitable for use in our system.

Overall for practical applications, the system design would need to balance the higher COD removal at the low flow rate (high HRT) with the cost of a larger reactor and any resultant power output.

It should be noted that our system design could not allow a flow-through mode, with flow through the granular anode bed, therefore the reactor was operated in flow-by mode, i.e. with AW flow across the face of the anode bed (opposite the cathode). Thus, with this configuration the mass transport of COD substrate in the anode was relatively low, particularly as the flow in the open section of the MFC would be laminar (with a Reynolds number <1.0), thus leading to mass transport in the anode bed mainly due to molecular diffusion. Directing the flow through the anode would increase the power output, as previously demonstrated [27,34].

Table 5 and Fig. 6 report the results obtained for inlet CODs of 50, 200 and 500 ppm, at the HRT of 446 min. When the inlet COD was increased from 50 to 200 ppm the percentage of COD removed decreased from 89% to 69%, whilst the effect on the Coulombic efficiency were minor, with a decrease of only 7% (from 68% to 63%). On the contrary, when the loading rate was increased to 161 kg COD $m^{-3}\ day^{-1}$ (500 ppm inlet COD), the effect on the Coulombic efficiency were higher, with a 22% decay with respect

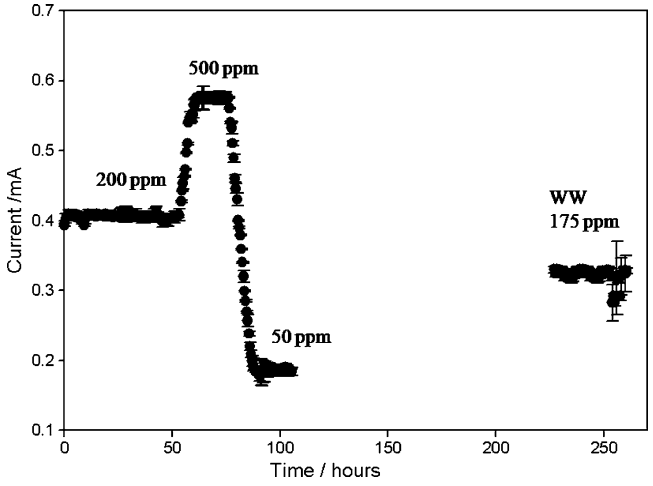

Fig. 6. Effect of the loading rate on SCMFC performance: variation of current with time. Anode: graphite granules (3 cm layer). Numbers indicate the inlet COD concentration of the AW utilized to feed the SCMFC. R_{ext}: 500 Ω. Error bars refer to two reactors.

to an inlet COD of 200 ppm. The percentage of COD removal also decreased by half compared to the case of a COD loading rate of 16 kg COD $m^{-3}\ day^{-1}$.

As for the case of operation in batch mode, the increase in the inlet COD corresponded to an increase in power output, and in particular the increase was linear: for an inlet COD of 500 ppm, the power output was 10 times higher than a feed COD of 50 ppm.

Zhang et al. [29], have recently reported the power performance of the MFC using a graphite packed bed anode and a pure culture (*K. pneumoniae* strain 117) of 466 mW m^{-3} based on the volume of a cube cell. This performance was equivalent to a power density of 172 mW cm^{-2} based on the cross-sectional area of the cathode 11.5 cm^2. They also increased the volumetric power density of the MFC by a factor of 7 (3773 mW m^{-3}) using a tube cell, although the cathode area was increased by an order of magnitude. Essentially the performance of both cells was similar based on the cathode area used.

The performance of the MFC of Zhang et al., operated under similar flow conditions in this work was similar (160 mW cm^{-2} vs 172 mW cm^{-2}) to that achieved in this work although we used a mixed microbial culture, not a pure culture.

From these data we can envisage a system of staged reactors, as it has been previously suggested. The wastewater at high COD loading rate fed to MFCs connected in series (or in a MFC cell stack), would undergo large reduction in COD (e.g. from 500 to 5 ppm), moreover, linking MFCs together would result in a nearly additive increase in total voltage [22,35].

Table 5
Effect of the COD loading rate on the SCMFC performance. Graphite granule bed depth: 3 cm. Flow rate: 0.0028 $cm^3\ min^{-1}$. R_{ext}: 500 Ω.

Fuel	Inlet COD, ppm	COD loading rate kg COD, $m^{-3}\ day^{-1}$	COD outlet at the steady-state, ppm	COD removal, %	Current output at the steady-state, mA	Power output at the steady-state, mW	Coulombic efficiency, %
AW	50	16	5.5 ± 2	89 ± 3	0.18 ± 0.02	0.016 ± 0.005	68 ± 7.2
AW	200	32.3	62 ± 14	69 ± 5.2	0.413 ± 0.007	0.085 ± 0.004	63 ± 4.5
AW	500	161	295 ± 60	41 ± 8.5	0.57 ± 0.04	0.163 ± 0.032	49 ± 2.7
WW	175	56	26.2 ± 10	85 ± 4.1	0.32 ± 0.3	0.096 ± 0.013	35 ± 11

Another interesting option would be to integrate the MFC technology with other technologies which are well established in wastewater treatment, such as anaerobic digestion [13,36].

The plant would include a prior anaerobic digestion to treat high COD effluent and a secondary treatment based on MFC to remove the residual organic carbon.

To simulate the performance of the SCMFCs with a granule bed depth of 3 cm in a treatment plant, sewage wastewater after primary clarify was fed to the system at a flow rate of 0.0028 cm^3. The wastewater had a COD of 175 ppm, resulting in a COD loading rate of 56 kg COD m^{-3} day^{-1}.

Table 5 reports the results obtained. Surprisingly, the current and power output were comparable with those of the AW at similar inlet COD. Moreover, the effluent treatment was very good, with a COD removal of 85%, close to the value obtained with AW at a COD loading rate of 16 kg COD m^{-3} day^{-1}. However, most of the COD removed did not lead to energy production: the Coulombic efficiency decreased, in fact, to $35 \pm 11\%$. This decrease might be associated with the presence in the sewage wastewater of alternatives electron acceptors, thus reducing the electron transfer at the anode [21].

Current output produced by the SCMFCs was stable (Fig. 6). Over the duration of the tests in continuous mode at the fixed HRT (around 11 days) the current output standard deviation was 0.0034 mA. This stability also was observed with real wastewater for which a standard deviation of 0.0097 mA in the current output was observed.

4. Conclusions

The use of a packed bed of irregular graphite granules as the anode on the performance of a single chamber microbial fuel cell (SCMFC) using an air cathode was demonstrated. This approach represents a low cost option for MFCs. In batch mode, the current output was found to increase with increase in thickness of the anode bed and with the approximate anode area. Scaling up from a flat sheet to a higher surface area packed bed did not produce a corresponding increase in current due to issues of current distribution and also mass transport limitations. Coulombic efficiencies varied from 30% to 80%, depending upon feed COD. In continuous mode operation, COD removal was 89% and Coulombic efficiency 68% with a feed of artificial wastewater (50 ppm as COD and volumetric power density of 1.3 W m^{-3}), with respect to the net anodic volume (12.5 cm^3) was achieved. Comparable performance was achieved with real wastewater and, notably, over the duration of tests current output was stable. Performance improvements can be achieved by modifying the flow within the packed bed electrode.

Acknowledgements

This work was supported by the European Union for Transfer of Knowledge award on biological fuel cells (contract MTKD-CT-2004-517215) and Northumbria Water.

We thank Northumbria Water for providing anaerobic sludge and wastewater from the primary clarifier from Cramlington WWTP.

References

[1] K. Rabaey, W. Verstraete, Microbial fuel cells: novel biotechnology for energy generation, Trends in Biotechnology 23 (2005) 291–298.
[2] D. Call, B.E. Logan, Hydrogen production in a single chamber microbial electrolysis cell (MEC) lacking a membrane, Environmental Science and Technology 42 (2008) 3401–3406.
[3] S. Cheng, B.E. Logan, Sustainable and efficient biohydrogen production via electrohydrogenesis, Proceedings of the National Academy of Sciences 104 (2007) 18871–18873.
[4] K. Rabaey, K. Van de Sompel, L. Maignien, N. Boon, P. Aelterman, P. Clauwaert, L. De Schamphelaire, H.T. Pham, J. Vermeulen, M. Verhaege, P. Lens, W. Verstraete, Microbial fuel cells for sulfide removal, Environment Science and Technology 40 (2006) 5218–5224.
[5] M. Di Lorenzo, T.P. Curtis, I.M. Head, K. Scott, A single chamber microbial fuel cell as a biosensor for wastewaters, Water Research 43 (2009) 3145–3154.
[6] I.S. Chang, H. Moon, J.K. Jang, B.H. Kim, Improvement of a microbial fuel cell performance as BOD sensor using respiratory inhibitors, Biosensors and Bioelectronics 20 (2005) 1856–1859.
[7] B.H. Kim, I.S. Chang, G.C. Gil, H.S. Park, H.J. Kim, Novel BOD sensor using mediator-less microbial fuel cell, Biotechnology Letters 25 (2003) 541–545.
[8] B.H. Kim, H.J. Kim, M.S. Hyun, H.S. Park, Direct electrode reaction of Fe(III)-reducing bacterium, *Shewanella putrefaciens*, Journal of Molecular Microbiology and Biotechnology 9 (1999) 127–131.
[9] H.J. Kim, H.S. Park, M.S. Hyun, I.S. Chang, M. Kim, B.H. Kim, A mediator-less microbial fuel cell using a metal reducing bacterium, *Shewanella putrefaciens*, Enzyme and Microbial Technology 30 (2002) 145–152.
[10] Y. Choi, E. Jung, H. Park, S.R. Paik, S. Jung, S. Kim, Construction of microbial fuel cells using thermophilic microorganisms, *Bacillus licheniformis* and *Bacillus thermoglucosidasius*, Bulletin of the Korean Chemical Society 25 (2004) 813–818.
[11] J.C. Biffinger, J. Pietron, R. Ray, B. Little, B.R. Ringeisen, A biofilm enhanced miniature microbial fuel cell using *Shewanella oneidensis* DSP10 and oxygen reduction cathodes, Biosensors and Bioelectronics 22 (2007) 1672–1679.
[12] K. Rabaey, N. Boon, S.D. Siciliano, M. Verhaege, W. Verstraete, Biofuel cells select for microbial consortia that self-mediate electron transfer, Applied and Environmental Microbiology 70 (2004) 5373–5382.
[13] T.H. Pham, K. Rabaey, P. Aelterman, P. Clauwaert, L. De Schamphelaire, N. Boon, W. Verstraete, Microbial fuel cells in relation to conventional anaerobic digestion technology, Engineering in Life Sciences 6 (2006) 285–292.
[14] K. Rabaey, G. Lissens, S.D. Siciliano, W. Verstraete, A microbial fuel cell capable of converting glucose to electricity at high rate and efficiency, Biotechnology Letters 25 (2003) 1531–1535.
[15] Y. Zuo, S. Cheng, D. Call, B.E. Logan, Tubular membrane cathodes for scalable power generation in microbial fuel cells, Environmental Science and Technology 41 (2007) 3347–3353.
[16] K. Rabaey, P. Clauwaert, P. Aelterman, W. Verstraete, Tubular microbial fuel cells for efficient electricity generation, Environmental Science and Technology 39 (2005) 8077–8082.
[17] B.E. Logan, S. Cheng, V. Watson, G. Estadt, Graphite fiber brush anodes for increased power production in air-cathode microbial fuel cells, Environmental Science and Technology 41 (2007) 3341–3346.
[18] D.H. Park, J.G. Zeikus, Improved fuel cell and electrode designs for producing electricity from microbial degradation, Biotechnology and Bioengineering 81 (2003) 348–355.
[19] B.E. Logan, J.M. Regan, Electricity-producing bacterial communities in microbial fuel cells, Trends in Microbiology 14 (2006) 512–518.
[20] B.E. Logan, Microbial Fuel Cells, Wiley, 2008.
[21] R.A. Rozendal, H.V.M. Hamelers, K. Rabaey, J. Keller, C.J.N. Buisman, Towards practical implementation of bioelectrochemical wastewater treatment, Trends in Biotechnology 26 (2008) 452–459.
[22] P. Aelterman, K. Rabaey, T.H. Pham, N. Boon, W. Verstraete, Continuous electricity generation at high voltage and currents using stacked microbial fuel cells, Environmental Science and Technology 40 (2006) 3388–3394.
[23] J. Heilmann, B.E. Logan, Production of electricity from proteins using a single chamber microbial fuel cell, Water Environment Research 78 (2006) 531–537.
[24] S.K. Chaudhuri, D.R. Lovley, Electricity generation by direct oxidation of glucose in mediatorless microbial fuel cells, Nature Biotechnology 21 (2003) 1229–1232.
[25] Z. He, S. Minteer, A. Angenent, Electricity generation from artificial wastewater using an upflow microbial fuel cell, Environmental Science and Technology 39 (2006) 5262–5267.
[26] Z. He, N. Wagner, S. Minteer, A. Angenent, An upflow microbial fuel cell with an interior cathode: assessment of the internal resistance by impedance spectroscopy, Environment Science and Technology 39 (2005) 5262–5267.
[27] P. Aelterman, M. Versichele, M. Marzorati, N. Boon, W. Verstraete, Loading rate and external resistance control the electricity generation of microbial fuel cells with different three-dimensional anodes, Bioresource Technology 99 (2008) 8895–8902.
[28] H. Liu, S. Cheng, L. Huang, B.E. Logan, Scale-up of membrane-free single-chamber microbial fuel cells, Journal of Power Sources 179 (2008) 274–279.
[29] L. Zhang, C. Liu, L. Zhuang, W. Li, S. Zhou, J. Zhang, Manganese dioxide as an alternative cathodic catalyst to platinum in microbial fuel cells, Biosensors and Bioelectronics 24 (2009) 2825–2829.
[30] A. Greenberg, L.S. Clesceri, A.D. Eaton, Standard Methods for the Examination of Water and Wastewater, 18th ed., Washington, 1992.
[31] A.D. Eaton, A. Greenberg, L.S. Clesceri, Standard Methods for the Examination of Water and Wastewater, 21st ed., American Public Health Association, American Water Works Association, Water Environment Federation, Washington, DC, 2005.
[32] K. Scott, Electrochemical Reaction Engineering, Elsevier Academic Press, London, 1991.

[33] B.E. Logan, B. Hamelers, R. Rozendal, U. Schröder, J. Keller, S. Freguia, P.S. Aelterman, W.K.R. Verstraete, Microbial fuel cells: methodology and technology, Environment Science and Technology 40 (2006) 5181–5192.
[34] S. Cheng, H. Liu, B.E. Logan, Increased power generation in a continuous flow MFC with advective flow through the porous anode and reduced electrode spacing, Environment Science and Technology 40 (2006) 2426–2432.
[35] S.E. Oha, B.E. Logan, Voltage reversal during microbial fuel cell stack operation, Journal of Power Sources 167 (2007) 11–17.
[36] P. Aelterman, K. Rabaey, P. Clauwaert, W. Verstraete, Microbial fuel cells for wastewater treatment, Water Science & Technology 54 (2006) 9–15.